



Adsorption of heavy metals from aqueous solution by magnetite nanoparticles and magnetite-kaolinite nanocomposite: equilibrium, isotherm and kinetic study

M.R. Lasheen^a, Iman Y. El-Sherif^a, Dina Y. Sabry^b, S.T. El-Wakeel^{a,*}, M.F. El-Shahat^b

^aWater Pollution Research Department, Environmental Research Division, National Research Centre, 33 El-Buhouth Street, Dokki, Cairo 12311, Egypt, Tel. +202 33371211; Fax: +202 33370931; emails: ragaei24@link.net (M.R. Lasheen), iman57us@yahoo.com (I.Y. El-Sherif), shaimaa_tw@yahoo.com, Shaimaa.tw@gmail.com (S.T. El-Wakeel)

^bFaculty of Science, Ain Shams University, Khalifa El-Maamon St, Abbasiya sq., Cairo 11566, Egypt, Tel. +202 26831474; Fax: +202 26847824; email: d.y_sabry@yahoo.com (D.Y. Sabry), Tel. +202 26831474; +202 26831231, Fax: +202 26847824; email: elshahatmf@hotmail.com (M.F. El-Shahat)

Received 9 January 2015; Accepted 13 August 2015

ABSTRACT

Nano magnetite (Fe₃O₄) and its composite with kaolinite were synthesized and tested for heavy metals (copper, lead, cadmium, chromium, and nickel) adsorption. The prepared magnetite–kaolinite (Mag-KL) nanocomposites were characterized by Transmission Electron Microscopy, powder X-ray diffraction, Fourier Transform Infrared spectroscopy, and the Brunauer–Emmett–Teller method. Various factors influencing the adsorption of metal ions such as contact time, initial metal concentration, pH, and the amount of adsorbent were investigated to optimize the operating conditions for the use of Mag-KL nanocomposites. The adsorption capacity of the magnetic composite increased with time. Adsorption reaches equilibrium in 120 min and the adsorption increases with the increase in pH. The composite was investigated for regeneration studies and the results confirmed that it could be reused for the adsorption of metal ions from aqueous solutions over five cycles without change in the sorption capacity.

Keywords: Magnetite; Kaolinite; Nanoparticles; Adsorption; Heavy metals

1. Introduction

Heavy metals are persistent environmental contaminants since they cannot be degraded or destroyed. The poisoning effects of heavy metals are due to their interference with the normal body biochemistry in the normal metabolic processes causing various diseases and disorders in living organisms [1–3]. Industrial, agricultural, urban and rural runoff, natural geological formations and household waste discharges directly or

indirectly into water sources cause excessive pollution of surface and underground water. Various treatment techniques and process have been used to remove the metallic ions from the wastewater, including precipitation, evaporation, solvent extraction, ion exchange, reverse osmosis, membrane separation, and so on. Most of these methods suffer from some drawbacks such as high capital and operational costs for the treatment and the disposal of the residual metal sludge [4].

In recent years, the synthesis and utilization of nano iron oxide have been widely studied, due to their nano size, superparamagnetism and the easy

*Corresponding author.

synthesis, coating, or modification [5]. Additionally, properties such as low toxicity, chemical inertness, high dispersion degree and biocompatibility, easy separation, and enhanced stability of magnetite nanoparticles have been reported [6].

All these properties make magnetite nanoparticles excellent candidates for combining metal binding and selective adsorption properties; and many laboratory studies indicated that magnetite nanoparticles in various forms could effectively remove a range of heavy metals, from water and wastewater solutions [7]. However, it is reported that nanomaterials tend to aggregate in solution [8]. Nanomaterials' stability can be enhanced, by their modification, based on the fact that nano iron oxide could react with different functional groups. The use of stabilizers, electrostatic surfactants, and steric polymers has been widely proposed for nanomaterial modifications [9]. It would be very interesting to synthesize magnetite nanoparticles composites and explore the effect of the composing materials on the ability of the nanoparticles for the removal of heavy metals. Clay minerals have high sorption, ion exchange, and expansion properties. Kaolinite is a kind of clay, which has many advantages such as wide sources, low cost, simple process, and easy use. In the present study, magnetite–kaolinite (Mag-KL) nanocomposites were prepared, gathering the adsorption features of kaolinite with the magnetic properties of nano magnetite to produce a magnetic adsorbent via chemical co-precipitation. The magnetic composite was further used for the removal of heavy metals. The adsorption capacity of metals by Mag-KL nanocomposites was compared to that of the prepared magnetite nanoparticles.

2. Materials and method

2.1. Materials

Ferric chloride hexahydrate ($\text{FeCl}_3 \cdot 6\text{H}_2\text{O}$), ferrous chloride tetrahydrate ($\text{FeCl}_2 \cdot 4\text{H}_2\text{O}$), ammonium hydroxide, nitric acid, copper sulfate ($\text{CuSO}_4 \cdot 5\text{H}_2\text{O}$), lead nitrate ($\text{Pb}(\text{NO}_3)_2$), and the chloride salts of Cd(II) and Ni(II) were of analytical grade and obtained from Aldrich, Germany. Kaolinite was obtained from Merck. All aqueous solutions were prepared with deionized water. The working solutions of metal ions were prepared by appropriate dilutions of the stock solution immediately prior to their use.

2.2. Synthesis of magnetite nanoparticles

Magnetite nanoparticles were prepared by co-precipitation method obtained according to

methodology previously described in other work [10] with average size 2–5 nm. In that method, Fe^{3+} and Fe^{2+} ions with 2:1 M ratio were dissolved in deionized water using anhydrous ferric chloride FeCl_3 and ferrous chloride tetrahydrate $\text{FeCl}_2 \cdot 4\text{H}_2\text{O}$.

Chemical precipitation was achieved by adding NH_4OH solution (25%) till a final pH of 10–12 was attained maintaining vigorous stirring for 2 h. The precipitates were heated to 80°C for 30 min, and then washed three times with distilled water and once with anhydrous ethanol. The particles were then dried in an oven at 70°C .

2.3. Synthesis of Mag-KL nanocomposite

Solutions of $\text{FeCl}_3 \cdot 6\text{H}_2\text{O}$ and $\text{FeCl}_2 \cdot 4\text{H}_2\text{O}$ at molar ratio 2:1 in 200 ml of deionized water were mixed with kaolinite. The amount of kaolinite was adjusted in order to obtain kaolinite: iron oxide weight ratios of 1:1. The solution was stirred at a rate of 200 rpm. Ammonium hydroxide solution was added to precipitate magnetite. Heat to 80°C , then dry in an oven at 80°C .

2.4. Characterization of adsorbents

The structural characterization of the prepared magnetite nanoparticles and Mag-KL was conducted by powder X-ray diffraction spectrometry (XRD) using Bruker D8 advance instrument. The instrument was equipped with a copper anode generating ($\text{Cu-K}\alpha$) radiation ($\lambda = 1.5406 \text{ \AA}$). All samples were recorded between 5° and 80° (2θ) at a scanning rate of $4^\circ/\text{min}$. Size investigation and morphology were identified by Transmission Electron Microscopy (TEM) using JOEL JEM (1230) electron microscope instrument with resolving resolution 0.2 nm. Gas adsorption analyzer with the Brunauer–Emmett–Teller method (Quantochrome NOVA Automated gas sorption systemsorb-1.12) was used for the surface area determination, where N_2 gas was used as adsorbate at 77 K. The functional groups of different adsorbents were identified by Fourier Transform Infrared Spectroscopy (FTIR) using FTIR-6100 (JASCO- Japan) instrument via the KBr pressed disc method, in a range starting from 400 to $4,000 \text{ cm}^{-1}$ wavenumbers.

Magnetic properties were measured in the solid state using a Vibrating Sample Magnetometer (VSM). The saturation magnetization value was determined from the plateau region of the magnetic flux density of a solid sample at 8,000.

2.5. Adsorption studies

The adsorption behavior of the prepared nano magnetite and Mag-KL nanocomposite for metal ions

(Cu²⁺, Pb²⁺, Cr(VI), Cd²⁺, and Ni²⁺) was investigated by means of the batch experiments at room temperature. The adsorption of Cr(VI) by magnetite nanoparticles was studied in another work [10]. A known amount of the adsorbent was mixed with a synthetic solution of Cu²⁺, Pb²⁺, Cr(VI), Cd²⁺, and Ni²⁺, separately in 20 mg/L for each metal ion. Batch adsorption experiments were conducted using different doses of the adsorbent ranging from 0.1 to 4 g/L of solutions containing heavy metal ions of desired concentrations (20 mg/L) for each metal ion.

The adsorption of metal ions by prepared magnetite nanoparticles was investigated in the pH range of 2–7. The solution pH was adjusted by 0.1 M NaOH and 0.1 M HNO₃. Samples were shaken in a rotary shaker at 200 rpm at different contact times ranging from 5 to 140 min. The equilibrium adsorption capacity, q_e (mg/g), of the metal was calculated using the mass balance, according to the following equation:

$$q_e = (C_o - C_e)V/m \quad (1)$$

Where V is the sample volume (L), m is the mass of the adsorbents (g), C_o is the initial metal ion concentration (mg/L), and C_e is the equilibrium concentration of metal ion in the solution (mg/L).

2.6. Analytical methods

The concentration of metal ions in the solution was determined according to APHA (2005) [11] using Atomic Absorption Spectrometer (Varian Spectra AAS 220) with graphite furnace accessory and equipped with deuterium arc background corrector. The precision of the metal measurement was determined by analyzing (in triplicate).

2.7. Desorption of metal ions and reusability of adsorbents

In this experiment, desorption of metals from metal-loaded nanoadsorbents was performed using 5 M HNO₃ solution. Mag-KL nanocomposite containing metals was exposed to 10 mL of 5 M HNO₃ and agitated at 200 rpm for 2 h. After desorption, the nanoadsorbent was separated by a small magnet followed by filtration and metal concentration measured. To test the reusability of the nanoadsorbents, 10 mL of 100 mg/L metal solution was mixed with 20 mg of adsorbents for 2 h and then desorbed with the addition of 10 ml of 5 M HNO₃, with stirring for 2 h. After each cycle of adsorption–desorption, the adsorbent was washed thoroughly with distilled water to

neutrality, then dried and reconditioned for adsorption in the succeeding cycle.

3. Results and discussion

3.1. Adsorbents characterization

TEM image for Mag-KL nanocomposite is shown in Fig. 1 and has a size of individual particles ranging within 7–11 nm.

The XRD pattern of magnetite-kaolinite composite is displayed in Fig. 2, there are several relatively strong flexion peaks in the 2θ region of 10–30°. The peak positions at diffraction angles of 30.1, 35.5, 43.1, 53.4, 57.0, and 62.6° proved the presence of magnetite. Peaks at 2θ of 12, 20, 22, 25, and 56° indicate the presence of kaolinite.

FT-IR spectra of Mag-KL nanocomposite, magnetite nanoparticles and kaolinite are compared in Fig. 3. As illustrated, the absorption band of Fe–O appeared at 537 cm⁻¹ for the composite. In the FT-IR spectra of kaolinite, the bands 3,621–3,960 cm⁻¹ correspond to stretching vibration of OH groups attached to octahedral layer of kaolinite. The Si–O stretching band in the 1,111 cm⁻¹, the Si–O–Si asymmetric stretching band in the 1,029 cm⁻¹, and the Si–O–Al bending band in the 537 cm⁻¹ are clearly seen. It was reported that the bands around 1,030 cm⁻¹ were due to the red clay origin of kaolinite [12]. The bands 1,112 cm⁻¹ and 1,029 cm⁻¹ are the most intense Si–O stretching modes and can be observed in most of silica minerals. The bands at 935 cm⁻¹ and 912 cm⁻¹ are attributed to hydroxyl vibration modes. The presence of magnetic nanoparticles can be seen by two strong absorption bands at around 467 and 720 cm⁻¹ [13].

Surface area of the prepared composite is 68.25 m²/g with total pore volume 0.027 cm³/g and average pore diameter 15.9 Å. The surface area

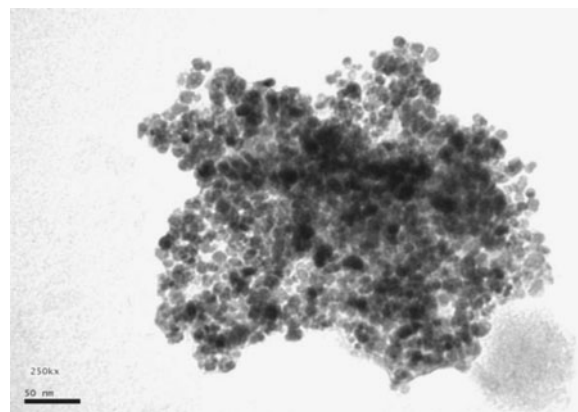


Fig. 1. TEM image of Mag-KL nanocomposite.

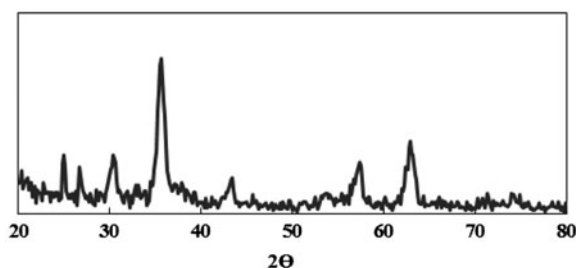


Fig. 2. XRD pattern of Mag-KL nanocomposite.

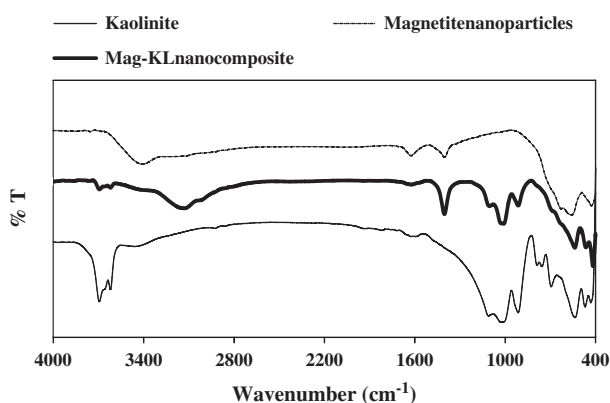


Fig. 3. FTIR chart of kaolinite, magnetite nanoparticles, and Mag-KL nanocomposite.

decreased compared to the surface area of magnetite nanoparticles ($125 \text{ m}^2/\text{g}$). The magnetic properties of Mag-KL nanocomposite decreased compared to the synthesized nano magnetite. Fig. 4 shows the hysteresis loops of the samples and the saturation magnetization was found to be 58.2 and 38.2 emu/g for nano magnetite and Mag-KL nanocomposite, respectively. Since the total iron concentration is constant in both prepared nano magnetite and Mag-KL nanocomposite, the decrease in saturation magnetization was due to the increased amount of kaolinite used in magnetite suspension, and its presence on the surface of magnetite nanoparticles creates a magnetically dead layer.

3.2. Sorption experiments

3.2.1. Effect of contact time

The results showed that the adsorption of the studied heavy metals shows gradual increase with the contact time and reaches equilibrium at 60 and 120 min using nano magnetite and Mag-KL nanocomposite, respectively. The composite showed comparable and less removal percentage to that obtained from nano

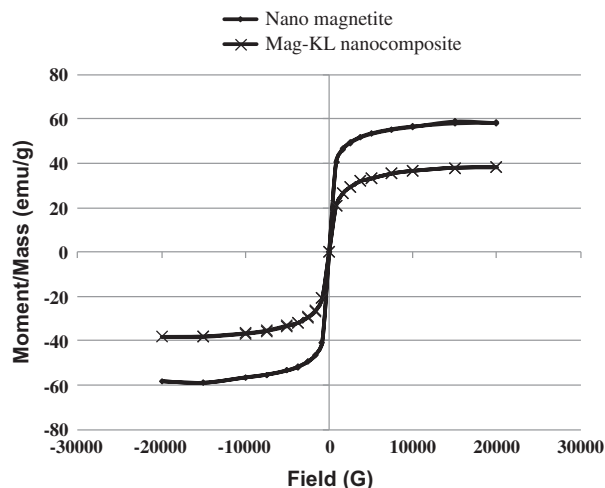


Fig. 4. VSM chart of nano magnetite and Mag-KL nanocomposite.

magnetite. The removal percentages were 95.8, 94, 92.8, and 92% for Cu^{2+} , Pb^{2+} , Cd^{2+} , and Ni^{2+} metal ions, respectively, using nano magnetite. The percentages were decreased to 90, 88, 85 and 83.2% for Cu^{2+} , Pb^{2+} , Cd^{2+} and Ni^{2+} ions respectively using Mag-KL nanocomposite.

3.2.2. Effect of initial pH

Results showed that the adsorption increased with increasing pH for all metals at initial metal ion concentration of 20 mg/L. Fig. 5(a) and (b) shows the effect of pH on the metal removal percentage of different metals using magnetite and Mag-KL nanocomposite.

The adsorption of metal ions onto the surface of iron oxide is likely to be an electrostatic attraction between the negatively charged surface of the iron oxide and the positive metal ions. Increasing the pH increases the surface deprotonation [14,15] which, in turn, results in the increase of the negatively charged sites. These charged sites enhance the attractive forces between the sorbent surface and metal ions [15]. Cu^{2+} removal increased to 98% at pH 5. The species of Cu influences its charge properties and likely uptake by magnetite. Overall, the dominant form of Cu at pH 2.0 is Cu^{2+} and with an increase in pH from 2.0 to 5.0, other species including $\text{Cu}_2(\text{OH})_2^{2+}$, $\text{Cu}(\text{OH})^+$, $\text{Cu}_2(\text{OH})^{3+}$, and $\text{Cu}_3(\text{OH})_4^{2+}$, are formed. The same thing happens to Pb(II), where the highest adsorption occurring at pH 6.5. Similar results were obtained by Nassar [16].

For pH above 5, adsorption experiments were not conducted for Cu and above pH 6.5 for Pb because of $\text{Pb}(\text{OH})_2$ and $\text{Cu}(\text{OH})_2$ precipitation [16].

The removal percentages of Cd^{2+} and Ni^{2+} gradually increased to 94 and 91%, respectively, using nano

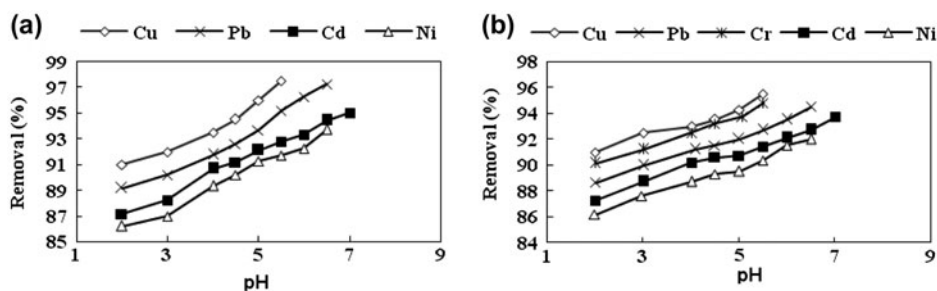


Fig. 5. Effect of initial pH on heavy metals removal by (a) magnetite nanoparticles and (b) Mag-KL nanocomposite.

magnetite with the pH increasing to 6.5 and 7. The removal percentages of Cd^{2+} and Ni^{2+} using Mag-KL gradually increased with increasing pH, but the removal is still less than that obtained from using nano magnetite. The dominant form of Ni is Ni^{2+} and at pH 4.0, the species $\text{Ni}(\text{OH})^-$ is formed [17]. At pH above 6.5, adsorption experiments were not conducted for nickel as the precipitation of nickel hydroxide was observed. Cadmium ions have a higher adsorption affinity to the nanoadsorbents than the ions of nickel. This affinity is related to a number of factors such as molecular mass, ion charges, ionic radius, hydrated ionic radius, and hydration energy of the metals.

3.2.3. Effect of adsorbent dose

As the adsorbent dosage increases, the adsorption increases. The removal of heavy metal ions increased with increasing composite and nano magnetite doses and equilibrium achieved at doses up to 2 g/L.

3.2.4. Desorption of metals and reusability of nano adsorbents

HNO_3 was used for the desorption of metals from Mag-KL nanocomposite and nano magnetite. Ten milliliters of 5 M HNO_3 was mixed with the metal mixture loaded adsorbents for 2 h. The desorption efficiencies for different metals were found to be 96 and 90% using nano magnetite and Mag-KL nanocomposite. After each cycle of adsorption–desorption, the adsorbents were washed thoroughly with distilled water to neutrality, then dried and reconditioned for adsorption in the succeeding cycle. The results show that the efficiencies of the recycled sorbents for removing metals are nearly the same as those for the fresh ones even after five times of recycling.

3.3. Adsorption isotherms

The Langmuir, Freundlich and Dubinin–Kaganer–Radushkevich (DKR) are the most common isotherm

models that describe the distribution of a metal ion between a solid and a liquid phase. Adsorption isotherms were obtained at optimum conditions of metal ion adsorption for the prepared adsorbents.

Fig. 6(a) and (b) shows the plot of Freundlich adsorption isotherm. The isotherm [18] suggests that the adsorption phenomenon occurred on heterogeneous surfaces. The isotherm assumes that the surface sites of the adsorbent have different binding energies and has the following form:

$$\log q_e = \log k_f + 1/n \log C_e \quad (2)$$

Where k_f , represents the adsorption capacity when metal ion equilibrium concentration equals to 1 (mg/g) and n is the degree of dependence of adsorption with equilibrium concentration. Freundlich parameters are shown in Table 1. The high R^2 values obtained are shown in the table.

The Freundlich constant ($1/n$) is related to the sorption intensity of the sorbent. When, $0.1 < 1/n < 0.5$, it is easy to adsorb; $0.5 < 1/n < 1$, there is some difficulty with the absorption; $1/n > 1$, there is quite a lot of difficulty with the absorption as stated by Treybal [19].

The values of $1/n$ were observed to be less than unity for all the adsorbents which suggests that the adsorption process is favorable.

The Langmuir isotherm [20] assumes monolayer coverage of the adsorption surface and no subsequent interaction among adsorbed molecules. Therefore, the adsorption saturates, and no further adsorption can occur. The isotherm can be represented in linear form by the following equation:

$$\frac{C_e}{q_e} = \frac{1}{bq_{\max}} + \frac{C_e}{q_{\max}} \quad (3)$$

q_{\max} is the maximum adsorption capacity at complete monolayer coverage (mg/g), b is the Langmuir

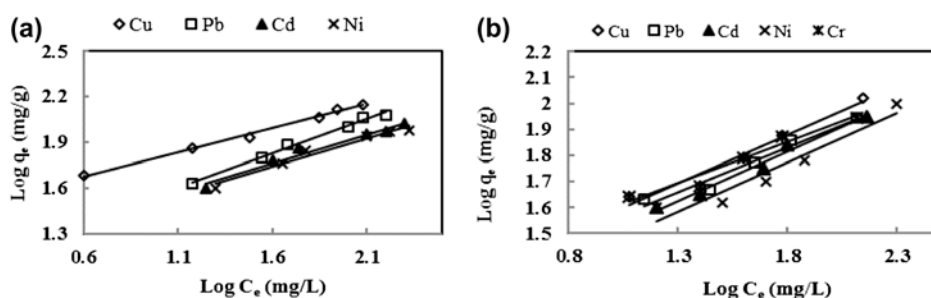


Fig. 6. Freundlich isotherm plots for metals adsorption by (a) magnetite nanoparticles and (b) Mag-KL nanocomposite (pH 5.5, contact time: 60, 120 min for magnetite nanoparticles and Mag-KL respectively, shaking rate: 200 rpm, amount of adsorbent: 2 g/L).

Table 1

Freundlich, Langmuir and DKR isothermal adsorption equation parameters for the adsorption of heavy metals by nano magnetite and Mag-KL nanocomposite at room temperature (adsorbent dose: 2 g/L, pH value: 5.5, metals concentration: 100–450 mg/L, contact time: 60, 120 min for magnetite nanoparticles and Mag-KL respectively, agitation speed: 200 rpm)

	Magnetite nanoparticles				Mag-KL nanocomposite				
	Pb ²⁺	Cu ²⁺	Cd ²⁺	Ni ²⁺	Pb ²⁺	Cu ²⁺	Cr(VI)	Cd ²⁺	Ni ²⁺
<i>Freundlich isotherm parameters</i>									
1/n	0.33	0.45	0.34	0.46	0.36	0.37	0.3	0.37	0.4
K _F (mg/g)	25.1	12.7	18.3	12.5	16.7	14.4	15.8	13.6	10
R ²	0.97	0.97	0.98	0.97	0.97	0.97	0.98	0.97	0.97
<i>Langmuir isotherm parameters</i>									
q _{max} (mg/g)	161.3	138	121	120	106	98	100	97	95.2
b (L/mg)	0.09	0.027	0.027	0.026	0.06	0.05	0.05	0.04	0.04
R ²	0.99	0.99	0.98	0.99	0.99	0.98	0.98	0.98	0.98
<i>DKR isotherm parameters</i>									
q _{max} (mol/g)	4 × 10 ⁻³	2.4 × 10 ⁻³	3.8 × 10 ⁻³	2.7 × 10 ⁻³	3 × 10 ⁻²	1.8 × 10 ⁻³	3.4 × 10 ⁻³	3 × 10 ⁻³	2 × 10 ⁻³
E (kJ/mol)	12	10.6	10.7	10.4	12.7	11	12.2	10.2	10
R ²	0.98	0.97	0.97	0.96	0.98	0.97	0.96	0.96	0.96

constant that relates to the heat of adsorption (L/mg). The adherence of adsorption data to Langmuir equation was tested and the results are shown in Table 1. These results suggest that Langmuir isotherm shows a good fit to the experimental data with well-matched correlation coefficients so that a heterogeneous distribution of active sites on the surface of the adsorbents occurs. The values of q_{max} obtained from the Langmuir model for metal ion adsorption on the composite are less than that from nano magnetite. It is reasonable to believe that the specific surface area gives an explanation for this behavior, since nano magnetite has a higher surface area than Mag-KL nanocomposite.

It has been reported that the maximum adsorption capacity values of different conventional materials such as Fly ash [21] and Sugar beet pulp [22] were 0.03 and 30.9 mg/g for Ni and Cu metal adsorption,

respectively. Adsorption capacity of nano magnetite for Ni, studied by Sharma et al. [23], was found to be 11.53 mg/g.

Magnetite nanoparticles of 8 nm size prepared by Shen et al. [24] have adsorption capacity of heavy metals of 35.46 mg/g at pH 4. Alginate and polyvinyl alcohol modified Fe₃O₄ with particle size 20 nm prepared by Li et al. [25] have an adsorption capacity 6.73 mg/g at pH 1. There are only few adsorption studies for Mag-KL nanocomposite.

The adsorption capacities of the prepared adsorbents as shown in Table 1 are high and the values were 161.3 and 120 mg/g for Pb²⁺ and Ni²⁺ using magnetite nanoparticles.

DKR isotherm model was applied for metal ions using the prepared adsorbents. The DKR isotherm model is valid at low concentration ranges and can be

used to describe adsorption on both homogeneous and heterogeneous surfaces. The general expression of the DKR isotherm [26] can be described by:

$$\ln q = \ln q_{\max} - \beta \varepsilon^2 \quad (4)$$

β is the activity coefficient related to mean sorption energy (mol^2/kJ^2), and ε is the Polanyi potential, which can be calculated from the next equation:

$$\varepsilon = RT \ln \left(1 + \frac{1}{C_e} \right) \quad (5)$$

where R is the ideal gas constant (8.3145 J/mol K), T is the absolute temperature (K).

The slope of the plot of $\ln q$ vs. ε^2 gives β (mol^2/J^2) and the intercept yields the maximum sorption capacity, q_{\max} (mol/g). E is defined as the free energy change (kJ/mol), which required transferring 1 mol of ions from solution to the solid surfaces. The relation is listed in the equation:

$$E = \frac{1}{\sqrt{-2\beta}} \quad (6)$$

The DKR parameters are listed in Table 1. The magnitude of E is useful for estimating the mechanism of the adsorption reaction. Adsorption is dominated by chemical ion exchange if E is in the range of 8–16 kJ/mol, whereas physical forces may affect the adsorption in the case of $E < 8 \text{ kJ/mol}$ [27]. The E values obtained from Eq. (8) are 12, 10.6, 10.4 and 10.3 for Cu^{2+} , Pb^{2+} , Cd^{2+} , and Ni^{2+} respectively using nano magnetite. The values were 12.7, 12.2, 11, 10.2 and 10 kJ/mol for Cu^{2+} , Pb^{2+} , Cr(VI) , Cd^{2+} , and Ni^{2+} respectively using Mag-KL nanocomposite. Values are in the adsorption energy range of chemical ion exchange reactions. This suggests that metal adsorption onto Mag-KL nanocomposite is attributed to chemical adsorption rather than physical adsorption.

3.4. Adsorption kinetics

Adsorption kinetics, demonstrating the solute uptake rate, is one of the most important characters which represent the adsorption efficiency of the composite and therefore, determines their potential applications. Adsorption kinetics samples were prepared by adding 10 mg of Mag-KL nanocomposite and nano magnetite to 5 ml solution at the effective pH value for each metal (20 mg/L). Approximately 60 and 120 min were enough to achieve the adsorption equilibrium using nano magnetite and Mag-KL

nanocomposite, respectively, under our experimental conditions.

The pseudo-first-order equation (Lagergren's equation) describes adsorption in solid-liquid systems based on the sorption capacity of solids [28]. The linear form of pseudo-first-order model can be expressed as:

$$\log(q_e - q_t) = \log q_e - \frac{k_1 t}{2.303} \quad (7)$$

where q_e and q_t are the amounts of adsorbed metals on the adsorbent at equilibrium and at time t , respectively (mg/g), and k_1 is the first-order adsorption rate constant (min^{-1}).

The calculated results of the first-order rate equation are given in Table 2. The q_e value acquired by this method contrasted with the experimental value. So the reaction cannot be classified as first-order.

Second-order kinetic equation was applied to find a more reliable description of the kinetics.

The pseudo-second-order kinetics can be represented by the following linear equation [29]:

$$\frac{t}{q_t} = \frac{1}{k_2 q_e^2} + \frac{t}{q_e} \quad (8)$$

where k_2 is the pseudo-second-order rate constant of adsorption (g/mg min).

Linear plot of t/q_t vs. t is achieved according to second-order kinetic equation (Fig. 7 (a) and (b)). The equation parameters calculated from the slope and intercept of the plot are summarized in Table 2. The calculated q_e values agreed very well with the experimental data. Since the correlation coefficients of the pseudo-second-order equation for the linear plots are very close to 1, the pseudo-second-order kinetics was a pathway to reach the equilibrium and the rate limiting step in heavy metals adsorption is chemisorption through the exchange of electrons between adsorbent and metal ions.

The Elovich kinetic model [30] is based on chemisorption phenomena and is expressed by equation:

$$\frac{dq}{dt} = \alpha \exp(-\beta qt) \quad (9)$$

Chien and Clayton [31] simplified the Elovich equation to the form:

$$q_t = \frac{1}{B} \ln(\alpha\beta) + \frac{1}{B} \ln(t) \quad (10)$$

where α (mg/g min) is the initial sorption rate and the parameter β (g/mg) is related to the extent of surface

Table 2

Kinetic parameters for the adsorption of heavy metals by nano magnetite and Mag-KL nanocomposite at room temperature (adsorbent dose: 2 g/L, pH value: 5.5, metals concentration: 20 mg/L, contact time: 60, 120 min for magnetite nanoparticles and Mag-KL respectively, agitation speed: 200 rpm)

	Nano magnetite				Mag-KL nanocomposite				
	Pb ²⁺	Cu ²⁺	Cd ²⁺	Ni ²⁺	Pb ²⁺	Cu ²⁺	Cr(VI)	Cd ²⁺	Ni ²⁺
<i>Pseudo-first-order</i>									
q_e (mg/g) (calculated)	10	4.8	5.1	3.3	3.6	4.8	5.1	3.3	3.2
q_e (mg/g) (experiment)	9.9	13.4	13	12	8	7.5	7	6.22	5.8
K_1 (min ⁻¹)	0.04	0.024	0.033	0.01	0.04	0.024	0.033	0.01	0.02
R^2	0.95	0.91	0.88	0.95	0.94	0.91	0.88	0.95	0.88
<i>Pseudo-second-order</i>									
q_e (mg/g) (calculated)	9	13.9	13.5	12	8.3	7.7	7.2	6.4	6
q_e (mg/g) (experiment)	8.8	13.4	13	12.4	8	7.5	7	6.22	5.8
K_2 (g/mg min)	0.04	0.01	0.01	0.01	0.02	0.035	0.03	0.04	0.03
R^2	0.99	0.99	0.99	0.99	80.9	0.99	0.99	0.99	0.99
<i>Elovich kinetic model</i>									
α (mg/g min)	276.4	13,261	372.4	1,483	280.9	828	85	413	50
β (g/mg)	0.78	1.01	0.82	1.04	0.78	1.56	1.3	1.78	1.5
R^2	0.92	0.95	0.94	0.93	0.92	0.95	0.94	0.93	0.92

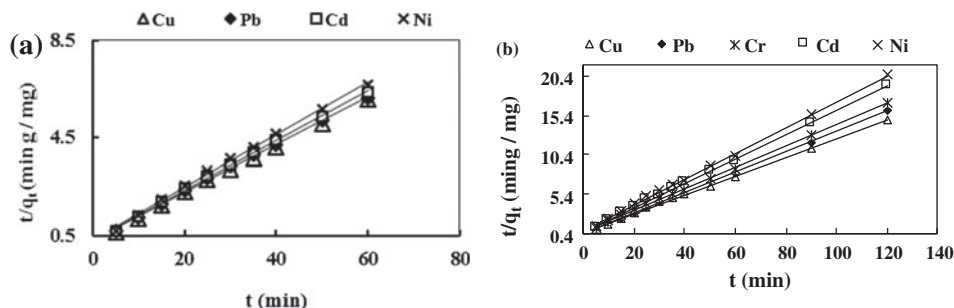


Fig. 7. Pseudo-second-order kinetics model of heavy metals adsorption by: (a) magnetite nanoparticles and (b) Mag-KL nanocomposite (adsorbent dose: 2 g/L, pH value: 5.5, initial concentration: 20 mg/L, contact time: 60, 120 min for magnetite nanoparticles and Mag-KL respectively, agitation speed: 200 rpm).

coverage and activation energy for chemisorption. The kinetic results will be linear on a q_t vs. $\ln(t)$ plot and the constants α and β can be computed from the slope and intercept of the graph. The kinetic constants obtained from the Elovich equation are listed in Table 2. The correlation coefficients obtained using the Elovich equation were lower than those of the pseudo-second-order equation. So, the Elovich equation might not be sufficient to describe the mechanism and the adsorption process is very fast, probably controlled by chemical adsorption.

4. Conclusion

Magnetite nanoparticles and their composite with Kaolinite were successfully synthesized using the

simple chemical co-precipitation method. Nanoparticles and the composite showed a high adsorption capacity for heavy metals with a super paramagnetism solving the problem of the adsorbed toxic metal separation from aqueous solutions.

The adsorption capacities of metal ions followed the order: $\text{Cu}^{2+} > \text{Pb}^{2+} > \text{Cr(VI)} > \text{Cd}^{2+} > \text{Ni}^{2+}$. The composite had a removal percentage less to some extent than pure nano magnetite. Adsorption by nano magnetite and Mag-KL nanocomposite attained equilibrium at 60 and 120 min, respectively, and was highly dependent on the solution pH and adsorbent dose. The adsorption data were well fitted by both the Langmuir and Freundlich isotherms and the pseudo-second-order kinetics. Sorption/desorption studies showed the possibility to reuse the composite and magnetite

several times for the sorption of copper, lead, chromium, cadmium, and nickel ions from aqueous solutions.

Acknowledgment

The authors thank the staffs of National Research Centre, Cairo, Egypt and heavy metals lab at Water Pollution Research Department, for their support.

References

- [1] I. Ghorbel-Abid, K. Galai, M. Trabelsi-Ayadi, Retention of chromium(III) and cadmium(II) from aqueous solution by illitic clay as a low-cost adsorbent, *Desalination* 256 (2010) 190–195.
- [2] A. Kouba, M. Buřič, P. Kozák, Bioaccumulation and effects of heavy metals in Crayfish: A review, *Water Air Soil Pollut.* 211 (2010) 5–16.
- [3] V.T.P. Vinod, R.B. Sashidhar, B. Sreedhar, Biosorption of nickel and total chromium from aqueous solution by gum kondagogu (*Cochlospermum gossypium*): A carbohydrate biopolymer, *J. Hazard. Mater.* 178 (2010) 851–860.
- [4] M.K. Jha, R.R. Upadhyay, J.C. Lee, V. Kumar, Treatment of rayon waste effluent for the removal of Zn and Ca using Indion BSR resin, *Desalination* 228 (2008) 97–107.
- [5] A.M.G.C. Dias, A. Hussain, A.S. Marcos, A.C.A. Roque, A biotechnological perspective on the application of iron oxide magnetic colloids modified with polysaccharides, *Biotechnol. Adv.* 29 (2011) 142–155.
- [6] F.L. Fan, Z. Qin, J. Bai, W.D. Rong, F.Y. Fan, W. Tian, X.L. Wu, Y. Wang, L. Zhao, Rapid removal of uranium from aqueous solutions using magnetic Fe₃O₄-SiO₂ composite particles, *J. Environ. Radioact.* 106 (2012) 40–46.
- [7] T.N. Morcos, S.S. Shafik, H.F. Ghoniemy, Self-diffusion of cesium ions in hydrous manganese dioxide from mixed solvent solutions, *Solid State Ionics* 167 (2003) 431–436.
- [8] C.L. Lin, C.F. Lee, W.Y. Chiu, Preparation and properties of poly (acrylic acid) oligomer stabilized superparamagnetic ferrofluid, *J. Colloid Interface Sci.* 291 (2005) 411–420.
- [9] Y.K. Sung, B.W. Ahn, T.J. Kang, Magnetic nanofibers with core (Fe₃O₄ nanoparticle suspension)/sheath (poly ethylene terephthalate) structure fabricated by coaxial electrospinning, *J. Magn. Magn. Mater.* 324 (2012) 916–922.
- [10] M.R. Lasheen, I.Y. El-Sherif, D.Y. Sabry, S.T. El-Wakeel, M.F. Shahat, Removal and recovery of Cr(VI) by magnetite nanoparticles, *Desalin. Water Treat.* 52 (2014) 6464–6473.
- [11] APHA, American Public Health Association, Standard Methods for the Examination of Water and Wastewater, twenty first ed., Washington, DC, 2005.
- [12] R. Palanivel, G. Velraj, FTIR and FT-Raman spectroscopic studies of fired clay artifacts recently excavated in Tamil Nadu, India, *Indian J. Pure Appl. Phys.* 45 (2007) 501–508.
- [13] M. Ma, Y. Zhang, W. Yu, H.Y. Shen, H.G. Zhang, N. Gu, Preparation and characterization of magnetite nanoparticles coated by amino silane, *Colloid Surf., A* 212 (2003) 219–226.
- [14] S.B. Johnson, G.V. Franks, P.J. Scales, D.V. Boger, T.W. Healy, Surface chemistry-rheology relationships in concentrated mineral suspensions, *Int. J. Miner. Process.* 58 (2000) 267–304.
- [15] P. Roonasi, A. Holmgren, An ATR-FTIR study of sulphate sorption on magnetite; rate of desorption, surface speciation, and effect of calcium ions, *J. Colloid Interface Sci.* 333 (2009) 27–32.
- [16] N. Nassar, Rapid removal and recovery of Pb(II) from wastewater by magnetic nanoadsorbents, *J. Hazard. Mater.* 184 (2010) 538–546.
- [17] X. Wang, J. Ren, H. Lu, L. Zhu, F. Liu, Q. Zhang, J. Xie, Removal of Ni(II) from aqueous solutions by nanoscale magnetite, *Clean-Soil Air Water* 38 (2010) 1131–1136.
- [18] H.M.F. Freundlich, Over the adsorption in solution, *J. Phys. Chem.* 57 (1906) 385–470.
- [19] R.E. Treybal, *Mass-Transfer Operations*, third ed., McGraw-Hill international, Singapore, 1981.
- [20] I. Langmuir, The constitution and fundamental properties of solids and liquids. Part I. Solids, *J. Am. Chem. Soc.* 38 (1916) 2221–2295.
- [21] M. Rao, A.V. Parwate, A.G. Bhole, Removal of Cr⁶⁺ and Ni²⁺ from aqueous solution using bagasse and flyash, *Waste Manage.* 22 (2002) 821–830.
- [22] E. Pehlivan, S. Cetin, B.H. Yanik, Equilibrium studies for the sorption of zinc and copper from aqueous solutions using sugar beet pulp and fly ash, *J. Hazard. Mater.* 135 (2006) 193–199.
- [23] Y.C. Sharma, V. Srivastava, Separation of Ni(II) ions from aqueous solutions by magnetic nanoparticles, *J. Chem. Eng. Data* 55 (2010) 1441–1442.
- [24] Y.F. Shen, J. Tang, Z.H. Nie, Y.D. Wang, Y. Ren, L. Zuo, Preparation and application of magnetic Fe₃O₄ nanoparticles for wastewater purification, *Sep. Purif. Technol.* 68 (2009) 312–319.
- [25] H.D. Li, Z. Li, T. Liu, X. Xiao, Z.H. Peng, L. Deng, A novel technology for biosorption and recovery hexavalent chromium in wastewater by bio-functional magnetic beads, *Bioresour. Technol.* 99 (2008) 6271–6279.
- [26] N.D. Hutson, R.T. Yang, Theoretical basis for the Dubinin-Radushkevitch (D-R) adsorption isotherm equation, *Adsorption* 3 (1997) 189–195.
- [27] Y.-M. Hao, M. Chen, Z.-B. Hu, Effective removal of Cu(II) ions from aqueous solution by amino-functionalized magnetic nanoparticles, *J. Hazard. Mater.* 184 (2010) 392–399.
- [28] Y.S. Ho, Citation review of Lagergren kinetic rate equation on adsorption reactions, *Scientometrics* 59 (2004) 171–177.
- [29] Y.S. Ho, Review of second-order models for adsorption systems, *J. Hazard. Mater.* 136 (2006) 681–689.
- [30] D.L. Sparks, *Kinetics of reaction in pure and mixed systems in soil physical chemistry*, CRC Press, Boca Raton, FL, 1986, pp. 12–18.
- [31] S.H. Chien, W.R. Clayton, Application of Elovich equation to the kinetics of phosphate release and sorption on soils, *Soil Sci. Soc. Am. J.* 44 (1980) 265–268.